2015 IEEE International Conference on Robotics and Automation (ICRA)
Washington State Convention Center
Seattle, Washington, May 26-30, 2015

Using Parallel Stiffness to Achieve Improved Locomotive Efficiency with the Sandia STEPPR Robot

Anirban Mazumdar[1], Steven Spencer[1], Jonathan Salton[1], Clinton Hobart[1], Joshua Love[1], Kevin Dullea[1], Michael Kuehl[1], Timothy Blada[1], Morgan Quigley[2], Jesper Smith[3], Sylvain Bertrand[3], Tingfan Wu[3], Jerry Pratt[3], and Stephen Buerger[1]

***Abstract*—In this paper we introduce STEPPR (Sandia Transmission-Efficient Prototype Promoting Research), a bipedal robot designed to explore efficient bipedal walking. The initial iteration of this robot achieves efficient motions through powerful electromagnetic actuators and highly back-drivable synthetic rope transmissions. We show how the addition of parallel elastic elements at select joints is predicted to provide substantial energetic benefits: reducing cost of transport by 30 to 50 percent. Two joints in particular, hip roll and ankle pitch, reduce dissipated power over three very different gait types: human walking, human-like robot walking, and crouched robot walking. Joint springs based on this analysis are tested and validated experimentally. Finally, this paper concludes with the design of two unique parallel spring mechanisms to be added to the current STEPPR robot in order to provide improved locomotive efficiency.**

I. INTRODUCTION

Recent disasters, both natural and manmade, have illustrated the need for robotic technologies to enter damaged or destroyed buildings, power-plants, and other infrastructures in order to search for survivors, investigate conditions, or shut down critical systems. For many of these applications, the robots must traverse terrain originally designed for humans such as stairs, ramps, and uneven surfaces. Therefore, bipedal robotic systems have emerged as one preferred solution, and the recent DARPA Robotics Challenge (DRC) Trials demonstrated several robot designs that successfully employ bipedal walking to navigate complex environments [1].

An ongoing challenge for bipedal robots is achieving high system level efficiencies. One convenient way to quantify efficiency is to use cost of transport (CoT). Cost of transport can be calculated using the energy consumed, E, distance traveled, d, and the mass m.

$$CoT = \frac{E}{mgd} \tag{1}$$

*This work was supported as part of DARPA's Maximum Mobility and Manipulation (M3) Program

[1]A. Mazumdar, S. Spencer, J. Salton, C. Hobart, J. Love, K. Dullea, M. Kuehl, T Blada, and S. Buerger are with Intelligent Systems, Robotics, and Cybernetics, Sandia National Laboratories, Albuquerque, NM, USA. amazumd@sandia.gov

[2]M. Quigley is with the Open Source Robotics Foundation, Mountain View, CA, USA. morgan@osrfoundation.org

[3]J. Smith, S. Bertrand, T. Wu and J. Pratt are with the BioInspired Robotic Lab at the Institute for Human and Machine Cognition (IHMC), Pensacola, FL, 32502, USA. jpratt@ihmc.us

Sandia National Laboratories is a multi-program laboratory managed and operated by Sandia Corporation, a wholly owned subsidiary of Lockheed Martin Corporation, for the U.S. Department of Energy's National Nuclear Security Administration under contract DE-AC04-94AL85000.

Thus far, only passive dynamic walking concepts have provided improved efficiency over human walking ($CoT = 0.2$) [2]. More versatile fully actuated bipedal robots still can only achieve a cost of transport that is an order of magnitude larger than humans [3]. This means that the ability to perform actual missions is severely restricted by battery life and size.

Our group is developing a novel bipedal robot, known as STEPPR (Sandia Transmission-Efficient Prototype Promoting Research), that attempts to achieve dramatic improvements in walking efficiency. This robot, shown in Fig. 1, uses a combination of powerful brushless DC motors and low transmission ratios (max of 10:1) at the leg joints to achieve highly back-drivable and efficient motions. While this is a multifaceted approach encompassing transmission design, walking control, and motor design, one key element is the use of elastic parallel elements to increase the efficiency of joint actuators.

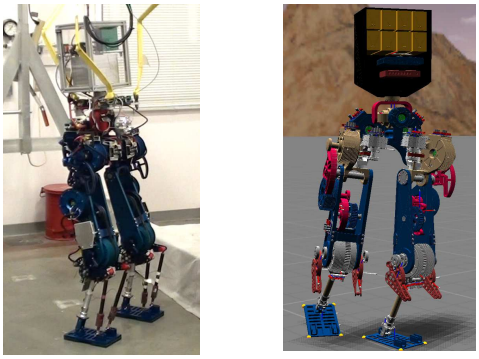

(a) STEPPR Standing in position control mode

(b) STEPPR walking in SCS environment.

Fig. 1. STEPPR holding a standing pose (a) and walking in Simulation Construction Set (SCS) environment (b).

It is well known that dynamic, bipedal, human-like walking includes spring-like energy storage and release at several leg joints [4]–[11]. Parallel spring elements at certain joints can be used to substantially reduce the torque output required of the joint motor, τ_m. The mechanical power at the joint remains the same, but electrical power dissipated by the motor is substantially reduced. Since the dissipated power is proportional to τ_m^2, reducing motor torque can play a critical role in increasing joint efficiency. In addition, by reducing the torques on the actuator output, the actuator and drive-train can be reduced in size. This would enable considerable savings in weight or could be used to increase robustness and fatigue life

of components.

Designs for passive protheses or robots have incorporated springs, as have active wearable assistive devices such as prosthetic ankles [5], or exoskeleton type suits [12], [13]. We apply similar concepts to the STEPPR robot.

In this paper we use a data driven approach to examine joint level behaviors across several bipedal walking gaits. This data illustrates that elastic elements can provide benefits across several types of gaits. These lessons are used to design parallel elastic systems for the STEPPR ankle, hip, and knee. Full scale parallel elastic elements are evaluated at the bench level. This work concludes with the presentation of "drop in designs" for the STEPPR robot which are predicted to provide substantial energy savings.

II. STEPPR Robot

The STEPPR robot was designed to serve as an efficient electromagnetic baseline robot testbed that supports the testing of gait-based interventions to provide even greater efficiency. STEPPR, shown in Fig. 1 and Fig. 2 includes six degrees of freedom per leg (hip adduction-abduction, flexion-extension and rotation; knee flexion-extension; and ankle dorsi-plantar flexion and inversion / eversion) as well as three rotational back joints.

All joints other than the ankles are driven with pure rotary actuators. Each ankle uses two rotary actuators that each drive a pushrod, providing a differential drive for the two ankle degrees of freedom. The pushrods form closed linkages that produce an effective gear ratio that varies by up to approximately 30 percent in the joint workspace. A close up view of the ankle linkage is provided in Fig. 2-b.

STEPPR was designed to use very high torque motors (Megaflux series from Allied Motion Technologies) with highly-efficient, low-reduction transmissions. Transmission ratios from motor to joint outputs range from $5-10$ for different joints. These modest gear reductions are implemented at each joint using a pair of pre-tensioned synthetic ropes that wrap around an input sheave and an output pulley. A photograph of this synthetic rope transmission is shown in Fig. 2-c. This arrangement produces a drive-train that has minimal losses and is intrinsically back-drivable. Back-drivability enables high quality torque control, which is critical for reducing impact forces and implementing dynamically-stable walking control, without spending extra drive energy to overcome intrinsic friction or inertia via torque feedback. Torque control is implemented open loop, with closed loop current control. Losses are dominated by Joule heating in the motors.

STEPPR is controlled by custom electronics designed for power efficiency. The idle power of the entire robot is $20W$ which consists of the power and data routing subsystems and the computational elements of the 15 joint controllers. When all joint level inverters are active and delivering zero current to the motors, the total robot power consumption rises to $50W$. STEPPR also allows for variable torso mass to simulate onboard batteries, computation, and other options. In its $75kg$ configuration, STEPPR requires just $100W$ ($1.5A$ at $65V$) to stand and support its own weight using joint position control. For walking control, STEPPR uses instantaneous capture point strategies developed at IHMC [14].

STEPPR was designed to allow the temporary installation of support elements at certain joints to increase total locomotive efficiency. Support elements could include parallel or series compliances, mechanisms that provide pose-dependent gear reductions, switchable transmissions, or other passive or active dynamic elements. Such elements may be designed using data from simulated and tested STEPPR gaits and implemented on the robot to verify energetic benefits.

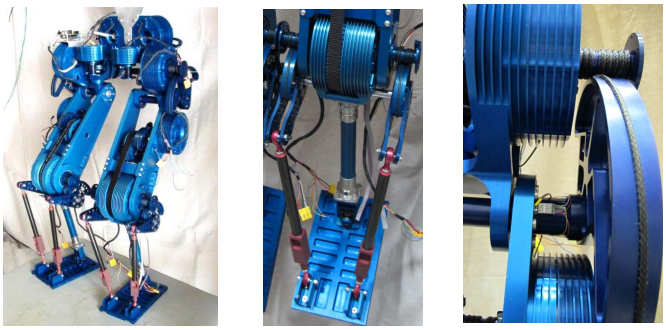

(a) Photo of STEPPR's 12 DOF Lower Body

(b) Close-up of differential ankle linkage

(c) Photo of STEPPR's rope transmission system

Fig. 2. Photograph of the STEPPR lower body illustrating the powerful DC motors and synthetic cable drive system.

III. Coordinate System

We begin by outlining the coordinate system used in this paper. We use the coordinate common to the robotics literature. The body coordinate frame, shown in Fig. 3, is centered at the pelvis, and the coordinate frame at each joint matches this overall convention. The hip rotations (black) are measured relative to the pelvis, the knee rotations (blue) are measured relative to the hip, and the ankle rotations (red) are measured relative to the knee. Throughout the paper we refer to rotations about the x, y, and z axes as roll, pitch and yaw respectively. Note that with this sign convention, spring-like behavior appears as a negative slope on the joint torque vs. angle curve. For consistency, all joint data described in this work are from the left leg.

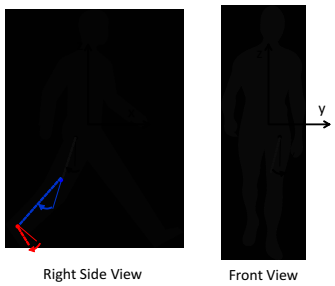

Fig. 3. An illustration of the coordinate system used throughout this work.

IV. Elastic Element Selection Approach

In this work we have analyzed three distinct data sets:

1) Human walking taken from human subjects [15].
2) Human-like robot walking simulations developed by the Institute for Human Machine Cognition (IHMC) for the Boston Dynamics ATLAS robot [16].
3) Conservative crouched gait simulations developed by IHMC for the Sandia STEPPR robot.

These three gaits provide the range of behaviors we predict for the STEPPR robot. Type 3 gaits are the motions generally associated with walking robots, slow and crouched gaits that allow the robot to maintain its balance. Type 2 gaits represent the results of advances in walking research with gaits becoming more dynamic and more similar to human gaits in speed and efficiency. This is a growing research field with several recent achievements [16]–[18]. Finally, type 1 gaits represent the "gold standard" for fully actuated bipedal walking. As gait algorithms and control strategies continue to evolve, we envision robots moving increasing towards type 1 gaits.

Our spring design approach is a sequential process. We begin by analyzing gait data joint by joint to roughly determine a parallel spring stiffness that provides benefit across all 3 gait types outlined above. Once this stiffness is determined, the gait data is again analyzed to determine the best zero location for the spring. This process must include several nuances because some gaits do not benefit from springs or do not benefit enough to influence the stiffness selection. In addition, most springs provide maximum energy benefit when unique behaviors such as selective engagement (during only a portion of the gait cycle) or unidirectional functionality are applied.

The key metric we attempt to minimize is joint motor energy consumption over the gait cycle. Since our actuators are brushless DC motors with high efficiency transmissions we use a simple DC motor model to estimate energy consumed. Specifically, we use the motor constant, K_m, the joint torque, τ_j, the joint speed ω_j, and the transmission reduction N.

$$E_m = \int \left(\frac{\tau_j(t)^2}{N^2 K_m^2} + \tau_j(t)\omega_j(t)\right)dt \tag{2}$$

The first term in the integrand represents Joule heating losses, and the second represents mechanical output energy. Other less significant loss elements are neglected for simplicity.

We illustrate the energetic benefits by comparing two cases for each gait. We use the term "uncompensated" to refer to the performance without the parallel elastic element, and we use the term "compensated" to refer to the performance with the parallel elastic element. In this paper we show how the energy consumption for the compensated case can be far lower than the uncompensated case.

While parallel elastic elements can substantially reduce energy consumption, different gaits that were not considered (such as climbing stairs or walking over rubble) can result in compensated torques that increase power consumption. In addition, the springs can also prevent maximum torque conditions from being reached in some pose configurations. We attempt to mitigate these by generally applying concepts that have shown commonality across three very different gaits. In addition, selective engagement and one-way engagement provide ways disengage the spring for unusual gaits or motions.

V. Ankle Pitch

During human-like walking, the ankle provides most of the power input to the system, and is known to benefit from a parallel spring [5]. Interestingly, all three gait types illustrate behaviors that benefit from a parallel spring. Plots of ankle torque vs. ankle angle for each gait are shown in Fig. 4.

Consider the case of the planted left foot for the human data in Fig. 4-a. As the body center of mass moves forward and causes the ankle to dorsiflex (negative pitch), the torque required to resist the falling of the body center of mass is positive and increases as the body falls further forward. A spring located at the ankle would therefore reduce the motor torque by providing a torque that increases with dorsiflexion. The human-like robot gait shows very similar behavior (4-b).

Note that this spring-like behavior only occurs during stance and not swing. Stance only springs have been proposed in prior works [7], [8], and for ankle discussions we will assume a spring that only engages during stance. With this stance-only behavior considered, Fig.4 shows that a spring with stiffness of roughly $400Nm/rad$ shows promise for all three gait types. Using the stiffness of $400Nm/rad$, the optimal zero location, x_0, was determined for each gait type. As Fig. 5 shows, this spring stiffness provides substantial energy reductions ranging from 48 to 77 percent.

VI. Hip Roll

Hip roll behavior also benefits from a parallel spring for all three gait types. The data in Fig. 6 shows that a one-way spring with stiffness $500Nm/rad$ provides clear benefits for all three gait types. In this case, the spring does not need the stance-only behavior of the ankle, making the overall design much simpler. The torque reductions provided by the $500Nm/rad$ parallel spring are illustrated in Fig. 7. This simple spring provides substantial energetic benefits, reducing the energy over a gait cycle by 40-90 percent.

VII. Hip Pitch and Knee Pitch

While ankle pitch and hip roll are the joints where parallel springs provide clear gains for all three gait types, hip and knee motions benefit from more tailored designs. For example, as shown in Fig. 8, a hip pitch spring with stiffness $72Nm/rad$ and zero position of $-0.35rad$ reduces the energy per cycle by 87 percent for the human gait. However, these benefits are not seen for gait types 2 or 3.

Similarly, a spring that acts to keep the knee out of hyperextension provides some benefit at the knee during the human-like robot gait. A spring with stiffness $200Nm/rad$ and zero position $0.2rad$ reduces the motor torques and allows the motor to harvest energy during the gait. The parallel spring

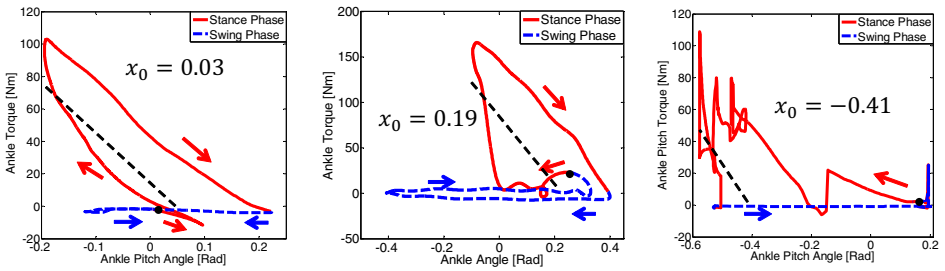

(a) Human Data (b) Human-like Robot Data (c) Crouched Robot Data

Fig. 4. Data showing the ankle torque vs. ankle position behavior for the three gait types. The black dot denotes the onset of ground contact, and the black dashed line represents the proposed $400Nm/rad$ spring. Ankle behavior is very spring-like during stance but not during swing.

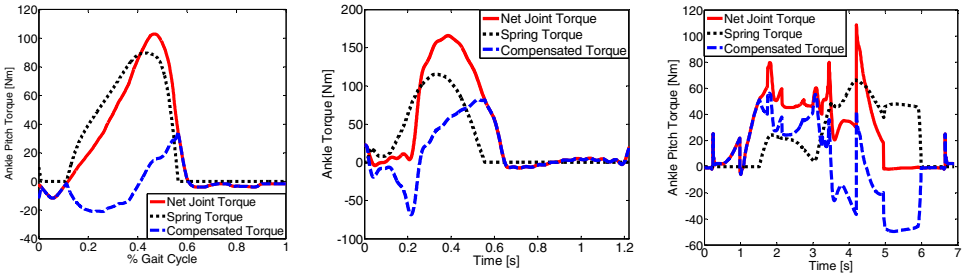

(a) Human Data (b) Human-like Robot Data (c) Crouched Robot Data

Fig. 5. Data showing the benefits of the $400Nm/rad$ ankle pitch parallel spring for the three gait types. Electrical energy is reduced by 77 percent (a), 62 percent (b), and 48 percent (c).

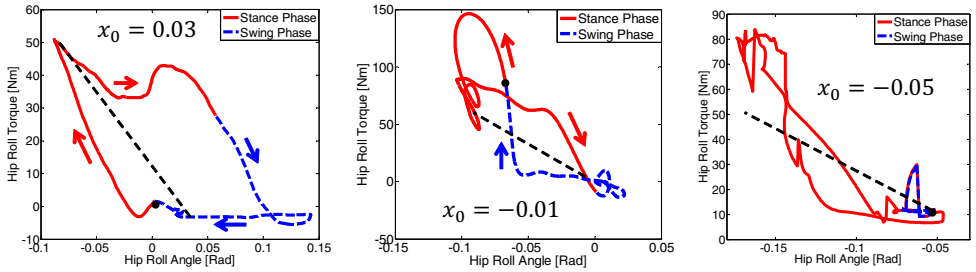

(a) Human Data (b) Human-like Robot Data (c) Crouched Robot Data

Fig. 6. Data showing the hip roll torque vs. hip roll position behavior for the three gait types. The black dot denotes the onset of ground contact, and the black dashed line represents the proposed $500Nm/rad$ spring. All three gait types exhibit spring-like behavior.

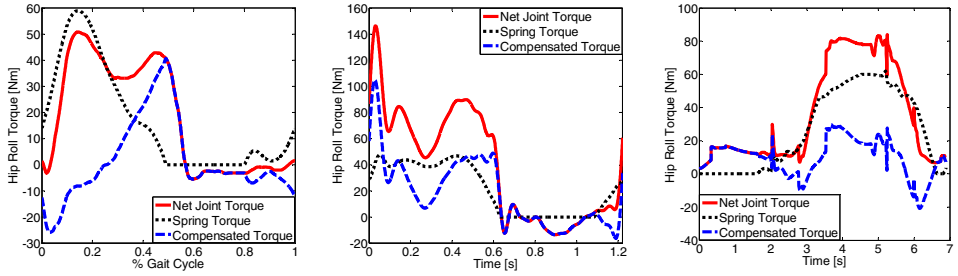

(a) Human Data (b) Human-like Robot Data (c) Crouched Robot Data

Fig. 7. Data showing the benefits of the $500Nm/rad$ parallel hip roll spring for the three gait types. Electrical energy is reduced by 40 percent (a), 75 percent (b), and 90 percent (c).

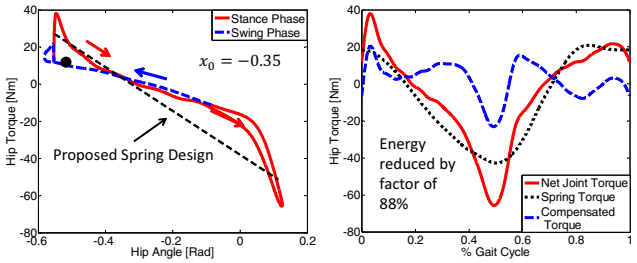

Fig. 8. Simulation showing hip pitch torque vs. hip pitch position (a) and the torque reduction when a $72Nm/rad$ parallel spring is used (b).

behavior is shown in Fig. 9. The spring reduces dissipated energy by $42J/cycle$ per leg.

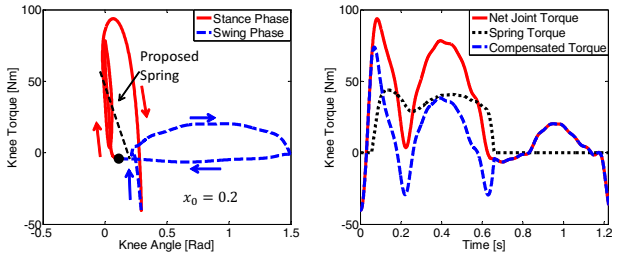

Fig. 9. Simulations based on human-like robot gait data illustrating the knee motion-torque profile (a) and the torque savings when a $200Nm/rad$ parallel spring is used (b).

VIII. Energetic Benefit Summary

The net energetic savings for each gait was calculated by combining the electrical energy at each joint (hip pitch, hip yaw, hip roll, knee pitch, ankle pitch). Each joint actuator model was determined using the STEPPR motor constants for that joint and the STEPPR gear reduction for the joint. The energy per cycle and predicted cost of transport for each of the three gait types is shown in Fig. 10. Note how the addition of elastic elements provides substantial reductions across all three gait types. Most importantly, this analysis predicts that the initial COT for STEPPR will be reduced from 3.34 to 2.16.

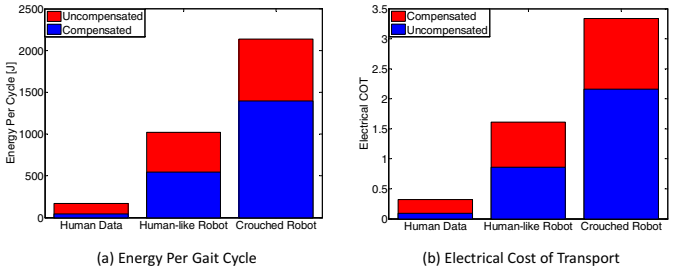

Fig. 10. Simulations illustrating the total energy per cycle (a) and predicted electrical cost of transport (b).

IX. Spring Design

Since the required springs must provide large torques and high torsional stiffness, we chose to use spiral torsion springs. The spiral torsion springs were designed using well known equations [19]. We assume the springs are made of spring steel ($E = 193GPa, \sigma_{yield} = 1200MPa$). The maximum moment, M, and travel, θ_s, can be computed from the gait data. The spring width, w, and thickness, t, (shown in Fig. 11-a) were selected to be $38mm$ and $4mm$ respectively in order to ease fabrication.

The active length, L, and the peak stress, σ_p can be computed using formulas based on bending [19].

$$L = \frac{Ewt^3\theta_s}{12M} \tag{3}$$

$$\sigma_p = \frac{6M}{wt^2} \tag{4}$$

Photographs of the springs are shown in Fig. 11-b. Note that two springs in parallel are used to achieve the desired ankle performance.

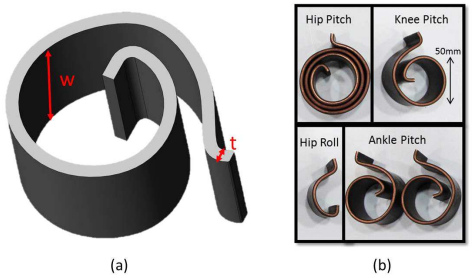

Fig. 11. Schematic diagram showing spiral spring dimensions (a) and photographs of the spring samples.

X. Bench Level Validation

In order to evaluate the spring designs and their underlying analysis, several characteristic trajectories were evaluated on a custom-built dynamometer. The system, shown in Fig. 12, consists of a large geared "trajectory motor" capable of rapid motions under large torques. The trajectory motor is connected through a torque sensor to the output of a synthetic rope transmission (6:1 ratio). The input of the rope transmission is connected to an Allied Motion Megaflux motor, identical to the hip pitch motor on STEPPR. We refer to this motor as the "torque motor." The trajectory motor operates in position control while the torque motor operates in torque control based on closed loop current control. The rope transmission is highly efficient and output torque roughly scales with current command to the torque motor. With this setup we can run joint trajectories from our simulated gaits and measure the ability of the torque motor to provide the desired torque while moving as it would during a gait. The phase currents into the torque motor are measured and are used to determine motor power dissipation. We use power dissipation rather than net motor

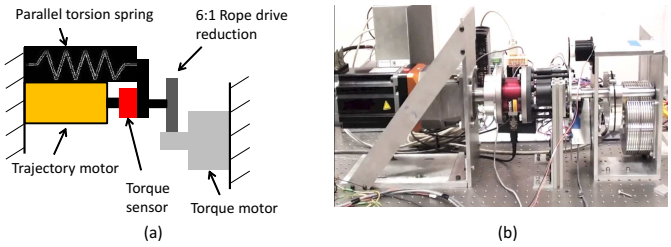

Fig. 12. Schematic diagram (a) and photograph (b) of the dynamometer setup.

power due to ease of measurement (motor voltages are noisy due to PWM switching).

The compensated case is evaluated by adjusting the torque motor torque trajectory to account for the behavior of the spring. The net joint torque (spring + motor) should match the uncompensated case, but the electrical power into the torque motor should reduce. We experimentally evaluated two characteristic trajectories with their specific springs: crouched robot hip roll, and human-like robot ankle pitch.

A. Crouched Robot Gait: Hip Roll

The results for the hip roll trajectory are shown in Fig. 13. This trajectory was evaluated at full load and full speed. As Fig. 13-a shows, the torque matches up well. The presence of the hip roll spring saves considerable power, reducing the dissipated power by 93 percent.

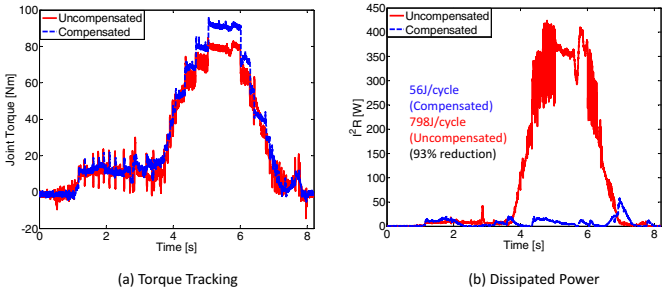

Fig. 13. Experimental data showing torque (a) and dissipated power (b) with and without a hip roll spring.

B. Human-like Robot Gait: Ankle Pitch

To account for limitations in the peak current of the dynamometer motor controller, the ankle pitch trajectory was scaled down by 25 percent. In addition, due to space constraints, only one of the two springs was used, resulting in a stiffness of $200Nm/rad$. Finally, this system did not include selective engagement. Therefore, the compensated stance and swing phases were performed separately and their data reassembled together in post-processing. The results in Fig. 14 show that even a single spring provides considerable reductions in dissipated power.

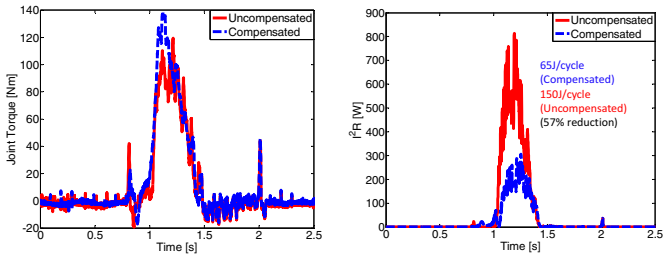

Fig. 14. Experimental data showing torque (a) and dissipated power (b) with and without an ankle pitch spring.

XI. Joint Specific Mechanism Design

With the effectiveness of the full scale spring designs confirmed for hip roll and ankle pitch, the final step is two design "kits" that allow them to mount onto the existing STEPPR design.

A. Hip Roll

The hip roll design is relatively straightforward because it does not require selective engagement. A rendering of the design is provided in Fig. 15-a. As the left leg rolls inward (negative roll angle), the green holder and the red tab come into contact with the spring. However, for motions in the positive roll direction, the spring provides zero torque. Adjustment for different gaits can be achieved by replacing the red engagement tab with longer or shorter pieces. This design has been fabricated and will be tested during real walking soon. A photograph of the prototype design attached to the back of STEPPR is shown in Fig. 15-b.

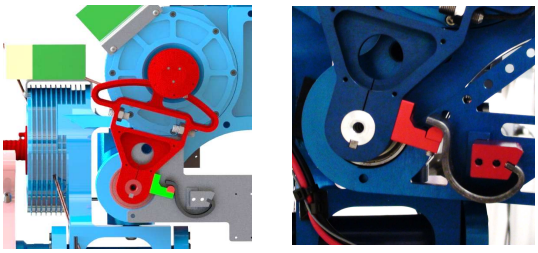

Fig. 15. A rendering (a) and photo (b) of the hip roll spring design.

B. Ankle Pitch

The ankle pitch design is considerably more challenging. This is due to the need for stance only engagement. While many approaches can be used for stance only engagement, we chose to use the force in the shank to activate the spring. Simulation data shows that the force in the shank quite large during stance ($\sim$ $700N$) but is near zero during swing. Therefore, we add a small amount of compliance to the shank and use this to activate an engagement mechanism for the

springs. In the absence of a large shank force, the springs remain disengaged.

A scale prototype of this design is shown in Fig. 16-a. In this design, a pneumatic heel pad is used to push a pair of pins into and out of contact with the spring engagement tab. This mechanism was validated on a scaled down dynamometer (1.4 percent torque, 50 percent speed). The results from this scaled test are shown in Fig. 17. The slow speed of the test allowed a subject to disengage the spring remotely by removing pressure from the pneumatic pad. Therefore in this test, the entire cycle (stance and swing) was performed at one time.

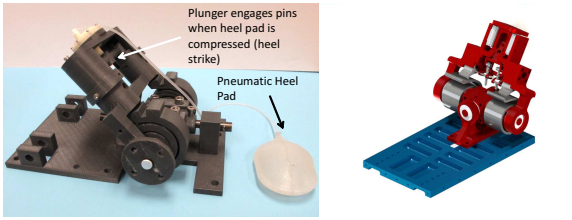

(a) Scaled Ankle Prototype (b) Rendering of Revised STEPPR Ankle

Fig. 16. A photograph (a) and rendering (b) of proposed ankle engagement designs.

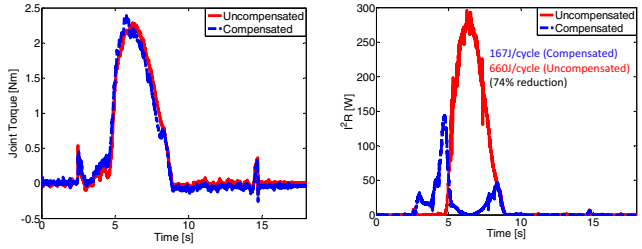

(a) Torque Tracking (b) Dissipated Power

Fig. 17. Experimental data from the scaled down ankle prototype.

These promising results were used to design a new ankle for STEPPR. This is intended as a drop in replacement for the existing ankle. A rendering of this design is shown in Fig. 16-b. Similar to the hip spring design, the spring zero position can be adjusted by swapping out engagement pawls.

XII. Conclusions

In this paper we have introduced a new bipedal robot designed for disaster response and with the specific goal of improving cost of transport. This robot, titled STEPPR, uses powerful brushless DC motors and efficient rope transmissions to achieve smooth, quiet, and highly backdrivable motions. We use three gait types to illustrate how parallel elastic elements can further improve the efficiency of the design for forward level walking. Specifically, a hip roll spring and an ankle pitch spring provide considerable benefits across the three very different gait types. Full scale springs were designed and validated experimentally. Finally, mechanisms were presented which allow these springs to be seamlessly incorporated into the existing STEPPR design.

Acknowledgment

The authors thank Greg Brunson and Nadia Coleman for their contributions to prototyping and testing.

References

[1] E. Ackerman. (2013, December) DARPA Robotics Challenge Trials: Final Results. IEEE Spectrum. New York City, NY. [Online]. Available: http://spectrum.ieee.org/automaton/robotics/humanoids/darpa-robotics-challenge-trials-results

[2] S. Collins, A. Ruina, R. Tedrake, and M. Wisse, "Efficient bipedal robots based on passive-dynamic walkers," *Science*, vol. 307, no. 5712, pp. 1082–1085, 2005.

[3] S. Cotton, I. Mihai, C. Olaru, M. Bellman, T. van der Ven, J. Godowski, and J. Pratt, "Fastrunner: A Fast, Efficient and Robust Bipedal robot. Concept and Simulation," in *Proc. IEEE International Conference on Robotics and Automation (ICRA'12)*, Minneapolis, MN, May 2012, pp. 2358–2364.

[4] J. Grimes and J. Hurst, "The Design of ATRIAS 1.0 a Unique Monoped, Hopping Robot," in *Proc. IEEE International Conference on Climbing and Walking Robots and Support Technologies for Mobile Machines)*, Baltimore, MD, 2012, pp. 548–554.

[5] S. Au, J. Weber, and H. Herr, "Powered Ankle–Foot Prosthesis Improves Walking Metabolic Economy," *IEEE Transactions on Robotics*, vol. 25, no. 1, pp. 51–66, 2009.

[6] R. Unal, S. Behrens, R. Carloni, E. Hekman, S. Stramigioli, and H. Koopman, "Prototype Design and Realization of an Innovative Energy Efficient Transfemoral Prosthesis," in *Proc. IEEE International Conference on Biomedical Robotics and Biomechatronics (Biorob'10)*, Tokyo, Japan, 2010, pp. 191–196.

[7] G. Folkertsma, S. Kim, and S. Stramigioli, "Parallel stiffness in a bounding quadraped with flexible spine," in *Proc. IEEE International Conference on Intelligent Robots and Systems (IROS'12)*, Vilamoura, Portugal, 2012, pp. 2210–2215.

[8] R. Unal, S. Behrens, R. Carloni, E. Hekman, S. Stramigioli, and H. Koopman, "Towards a Fully Passive Transfemoral Prosthesis for Normal Walking," in *Proc. IEEE International Conference on Biomedical Robotics and Biomechatronics (Biorob'12)*, Roma, Italy, 2012, pp. 1949–1954.

[9] K. Hollander, R. Ilg, T. Sugar, and D. Herring, "An efficient robotic tendon for gait assistance," *Journal of Biomedical Engineering*, vol. 128, no. 5, pp. 788–791, 2006.

[10] V. Duindam and S. Stramigioli, "Optimization of mass and stiffness distribution for efficient bipedal walking," in *2005 International Symposium on Nonlinear Theory and its Applications*, Tokyo, Japan, 2005, pp. 481–484.

[11] T. Yang, E. Westervelt, J. Schmiedeler, and R. Brockbrader, "Design and control of a planar bpedal robot ernie with parallel knee compliance," *Autonomous Robots*, vol. 25, pp. 317–330, 2008.

[12] A. Valiente, "Design of a Quasi-Passive Parallel Leg Exoskeleton to Augment Load Carrying for Walking," Master's thesis, Massachusetts Institute of Technology, Cambridge, 2005.

[13] A. Dollar and H. Herr, "Design of a Quasi-Passive Knee Exoskeleton to Assist Running," in *Proc. IEEE International Conference on Intelligent Robots and Systems (IROS'08)*, Nice, France, 2008, pp. 747–754.

[14] J. Pratt, T. Koolen, T. de Boer, J. Rebula, S. Cotton, J. C. M. Johnson, and P. Neuhaus, "Capturability-Based Analysis and Control of Legged Locomotion, Part 1: Theory and Application to M2V2, a Lower Body Humanoid," *International Journal of Robotics Research*, vol. 31, no. 10, pp. 1117–1133, 2012.

[15] A. Shache and R. Baker, "On the expression of joint moments during gait," *Gait and Posture*, vol. 25, pp. 440–452, 2007.

[16] J. Pratt and B. Krupp, "Design of a bipedal walking robot," in *Proceedings of the 2008 SPIE*, Tokyo, Japan, 2008, pp. 1–13.

[17] A. Ames, "Human-inspired control of bipedal walking robots," *IEEE Transactions on Automatic Control*, vol. 59, no. 5, pp. 1115–1130, 2014.

[18] D. Braun and M. Goldfarb, "A control approach for actuated dynamic walking in bipedal robots," *IEEE Transactions on Robotics*, vol. 25, no. 6, pp. 1292–1303, 2009.

[19] Springs and Things. (2002) Handbook of Spring Design. Spring Manufacturers Institute. Oak Brook, IL. [Online]. Available: http://www.springsandthings.com/pdf/spiral-torsion-springs.pdf